





Article

Assessment of Net Erosion and Suspended Sediments Yield within River Basins of the Agricultural Belt of Russia

Kirill Maltsev ^{1,*} , Valentin Golosov ^{1,2}, Oleg Yermolaev ¹ , Maxim Ivanov ¹  and Nelli Chizhikova ¹ 

¹ Department of Landscape Ecology, Institute of Ecology and Environment, Kazan Federal University, 420097 Kazan, Russia

² Institute of Geography Russian Academy of Science, 119017 Moscow, Russia

* Correspondence: mlcvkirill@mail.ru

Abstract: The SEA/Balance (soil erosion–accumulation balance) model and the WATEM/SEDEM model both mapping the erosion–accumulation budget of sediment within river basins were tested for 11 river basins of the eastern Russian Plain. The dynamics of river sediment yield were evaluated within one of the river basins. The analysis is based on observations of suspended sediment yield in test river basins with an area ranging from 100 to 1500 km². The maps of the average annual erosion–accumulative budget of sediment were constructed using two methods, making it possible to quantitatively assess the amount of sediment yield from the catchment area for the river basins under study. The WATEM/SEDEM model and the author’s SEA/Balance model were used for sediment yield estimation. The results of calculation using the WATEM/SEDEM model have an average bias of +11% compared to observed suspended sediment yield. The corresponding value in the case of the SEA/Balance model application is –29%. SEA/Balance model assessment sediment yield dynamics for the Sterlya river basin show an 11 percent reduction. It is possible to conclude that the proposed method of SEA/Balance can be applied to river basins of the agricultural zone of the east Russian Plain.



Citation: Maltsev, K.; Golosov, V.; Yermolaev, O.; Ivanov, M.; Chizhikova, N. Assessment of Net Erosion and Suspended Sediments Yield within River Basins of the Agricultural Belt of Russia. *Water* **2022**, *14*, 2781. <https://doi.org/10.3390/w14182781>

Academic Editor: Yeshuang Xu

Received: 3 August 2022

Accepted: 1 September 2022

Published: 7 September 2022

Publisher’s Note: MDPI stays neutral with regard to jurisdictional claims in published maps and institutional affiliations.



Copyright: © 2022 by the authors. Licensee MDPI, Basel, Switzerland. This article is an open access article distributed under the terms and conditions of the Creative Commons Attribution (CC BY) license (<https://creativecommons.org/licenses/by/4.0/>).

Keywords: WATEM/SEDEM; SEA/Balance; sediment delivery ratio; erosion–accumulative budget mapping

1. Introduction

The long-term quantitative assessment of erosion and accumulation intensity in a river basin, as well as the evaluation of sediment yield from a river basin into a river, are among the key indicators for determining the soil degradation rate in a river basin and the degree of streams pollution by sediment [1].

The erosion–accumulative processes are incredibly intensive in areas with a high degree of slope plowing. Thus, the quantitative assessment of erosion–accumulative processes on arable lands is an urgent task [2].

Significant climatic changes have occurred in the study region, as well as in the southern half of the European part of Russia over the past few decades (since the early 1990s). An increase in the frequency of intense rainfall has led to a slight rise in soil loss, and a sharp reduction in surface runoff during snowmelt has led to a large decrease in soil loss [3]. In addition, the areas of arable land have varied quite strongly, and the borders of the fields have changed, which has resulted in decreased erosion and sediment yield. [4,5]. At the same time, the river sediment yield observations network was significantly reduced. The use of the sediment spatial redistribution models verified and adapted for specific regions will make it possible to identify the hot points of the most significant basin erosion and potential sediment inflow into water objects.

Several multi-temporal cartographic models have been developed, representing either the degree of soil cover degradation from erosion processes or the intensity of erosion processes on arable land within the European territory of Russia. However, no

maps show the average annual erosion-accumulative sediment budget for the river basins integrally [6,7]. Creating a map reflecting the intensity of erosion along with accumulation would be very relevant for the study area.

Studies obtaining maps of the annual erosion-accumulation budget of deposits are rare. For example, the USPED model allows producing the erosion and accumulation maps for Washington State (USA) [8]. However, only qualitative analysis was conducted in this study, and there are no quantitative estimates of the sediment budget. In addition, a quantitative spatial model of the erosion-accumulation budget has been created within one of the river basins in Spain using the WATEM/SEDEM model [9,10]. A net water erosion map using the WATEM/SEDEM model was constructed as part of the research conducted in Mongolia in analyzing the contribution of gold mines to the sediment yield of the Tuul River. Spatial analysis showed that higher soil losses were obtained for slopes taken up by agricultural land. Sediment accumulation occurred mainly in the valley bottoms of the Tuul River tributaries, which are often located within or near the mining areas [11].

Erosion and accumulation processes can be evaluated using various methods and approaches described in the literature, but essential is the soil erosion models, which are currently implemented using GIS [12]. There are different classifications of erosion models. Most researchers identify conceptual, empirical, and physically based models [13].

At present, only a few empirical models are capable of estimating the average annual soil erosion losses. The most widely used are USLE [14] and its modifications RUSLE [15], RUSLE2 [16], and RUSLE3D [17]. The main advantage of these empirical models is the relatively easy access to data, and the main disadvantages are the lack of consideration of the accumulation of eroded soil on the slopes and soil losses from meltwater runoff. Mean annual estimates also make it possible to make models intended for the evaluation of soil erosion losses from runoff events. An example of such studies is the assessment of erosion and sediment yield carried out in the Danube river basin using the SWAT model [18].

To spatially assess the erosion-accumulative sediment budget within an area, it is necessary to know not only the eroded material amount but also how this material will accumulate along the sediment transport path from the slopes into the river network. The sediment connectivity of an area largely determines the processes of material accumulation down the slope [19].

Sediment connectivity can be evaluated using a variety of quantitative indicators. Sediment delivery ratio (SDR) [1] works on the assumption that only part of the soil washed away in the catchment area moves downslope and into the river network. Although this indicator was proposed a long time ago [19], it is still used in various studies [20–22].

One of the most widely used indicators for quantifying sedimentary connectivity is the index of connectivity (IC) [23]. This index has been applied in many different regions of the world: China [24]; France [25]; Spain [26]; Japan [27]; and Australia [28].

The researchers also use this indicator as the “delivery time” (travel time) of sediment from the territorial unit to the stream [28]. This approach has been implemented in the SEDD model [29] and applied in different parts of the world [30]. This indicator, like the previous one, needs calibration when used for new territory.

There is also a “transport capacity” indicator [31–33]. This indicator is implemented in the WATEM/SEDEM model. This model allows the spatial simulation of erosion-accumulative processes in river basins with the construction of a mean annual sediment budget map and the estimation of sediment outflow from the river basin, which allows a quantitative verification of the results by comparing with observed data [9–11,31–33]. The methodology is implemented in open access software (<https://ees.kuleuven.be/eng/geography/modelling/watemsedem2006/>, accessed on 15 July 2021) and requires a relatively small set of spatial data, making it very attractive. The model has been previously applied to the southwest of the European part of Russia (EPR). In particular, the digital mapping of soils and the degree of soil erosion within the Belgorod region have been performed and determined [33].

The WATEM/SEDEM methodology was dedicated to use within small river basins from few hectares to tens of square kilometers [34]. The model was initially developed for the natural conditions of Belgium. Thus, the model must be calibrated for use in the east of the Russian Plain. However, in our case, there are not enough initial data for this.

At the same time, there are quite a lot of field studies on small river basins of the EPR, which estimated the sediment delivery ratio. These estimates were used to identify several groups of small river basins depending on the features of the relief and made it possible to replace the sediment transport capacity in the WATEM/SEDEM model with group-averaged SDRs.

The goal of this study is to develop a methodology that implements spatial modeling of the average annual erosion–accumulative sediment budget for the eastern part of the Russian Plain and a comparative analysis with the WATEM/SEDEM methodology. The model under development was named SEA/Balance (soil erosion–accumulative balance). The proposed methodology was used to assess changes in sediment yield from the catchment area for one of the river basins over two time intervals that differ by climatic conditions and changes in land-use structure.

2. Materials and Methods

2.1. Study Area

Eleven small river basins of the east Russian Plain supplied with data on annual suspended sediment yield at the hydrological station were selected as study sites or test river basins (Figure 1).

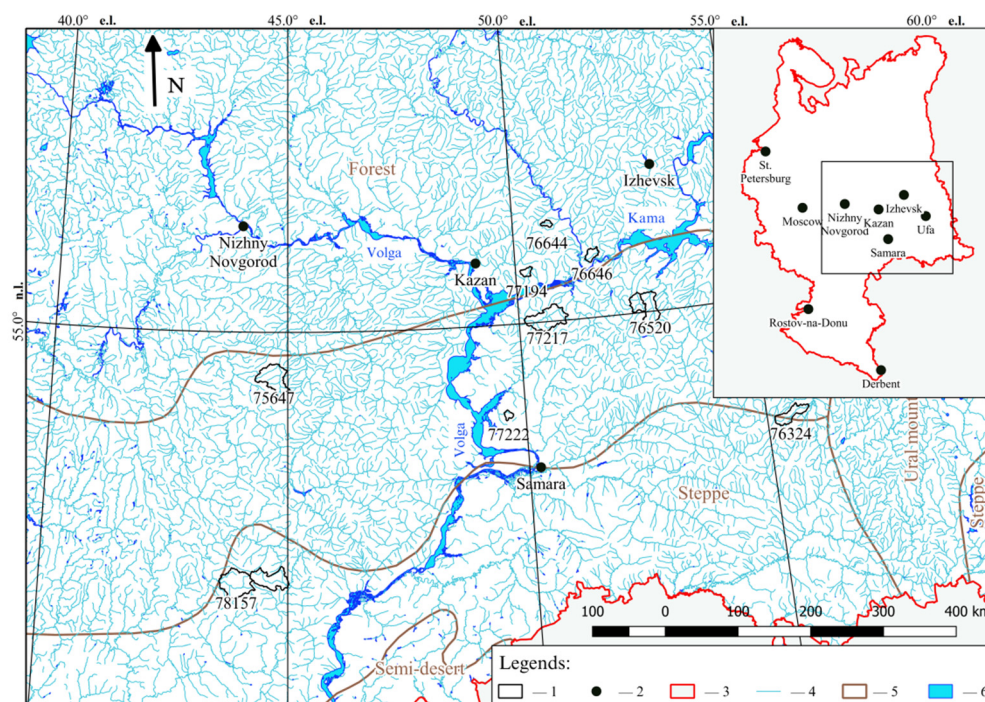


Figure 1. Location of test river basins (1—river basin boundaries, 2—cities, 3—border of the European territory of Russia, 4—rivers, 5—boundaries of landscape zones, 6—water bodies).

The selected basins are located within three landscape zones: forest; forest-steppe; steppe. According to the Unified State Register of Soil Resources [35], either gray forest soils (Greyic Phaeozems) or black soils (Chernozems) predominate within these river basins. The annual climatic parameters averaged over the period from 1966 to 2013 for the selected river basins are presented in Table 1 (the warm season is determined to be the time during which the average daily temperature is above 0 °C). Table 1 was created based on the data from the website of the Russian Research Institute of Hydrometeorological Information—World

Data Center (RIHMI-WDC) (<http://meteo.ru/>, accessed on 10 July 2021). The study area is characterized by average annual precipitation from 442 mm at the Oktyabrsky Gorodok climatic station to 551 mm at the Samara climatic station by the data from Table 1. The long-term average temperature varies from 3.1 °C at the Kilmez climatic station to 5.7 °C at the Rostashi climatic station.

Table 1. Mean annual climatic characteristics of test river basins.

River Basin ID	Nearest Climatic Station Name	P*—Warm Season, mm	P—Cold Season, mm	Mean Annual P, mm	T*—Warm Season, °C	T—Cold Season, °C	Mean Annual T, °C
77194	Kazan	361	187	548	12.7	−7.7	4.1
76644	Kilmez	389	153	542	11.7	−8.8	3.1
77217	Chulpanovo	336	146	482	12.7	−8.8	3.7
76324	Sterlitamak	335	185	520	13.1	−9.5	3.7
76522	Elabuga	361	177	538	12.7	−8.3	3.9
76520	Elabuga	361	177	538	12.7	−8.3	3.9
75647	Krasnoslobodsk	359	180	539	12.9	−6.9	4.6
78205	Oktyabrsky Gorodok	286	156	442	14.0	−6.9	5.3
78157	Rostashi	321	128	449	14.1	−6.0	5.7
76646	Elabuga	361	177	538	12.7	−8.3	3.9
77222	Samara	323	228	551	14.5	−7.0	5.6

Note(s): * T—temperature, P—precipitation.

The study area is characterized by slope steepness from 1.2 degrees in the Birla river basin (77222) to 2.6 degrees in the Betka river basin (77194). The studied river basins are characterized by a large proportion of cropland, which varies from 52% in the Betka river basin to 78% in the Atkarka river basin (Table 2).

Table 2. Relief and land use characteristics of test river basins affect the mass of formed sediment and its transport.

River Basin ID—River Name	Slope Angle, (deg)	Length of Slopes, (m)	Density of Dry Valley Network, (km/km ²)	Density of River Network, (km/km ²)	Cropland (%) of Catchment Area	Area (km ²)
77194—Betka river	2.6	175	0.96	0.61	52	141
76644—Nurminka river	2.3	133	0.52	0.57	69	96
77217—Malyy Cheremshan	1.5	174	0.55	0.23	65	1254
76324—Sterlya River (1985) y.	1.6	177	-	0.44	61	591
76324—Sterlya River (2018) y.	1.6	162	-	-	56	591
76522—Menzelia river	2.3	209	0.52	0.65	71	396
76520—Mellya river	2.1	218	0.60	0.26	66	766
75647—Rudnya river	2.3	200	-	0.26	63	1136
78205—Atkarka river	1.8	176	-	0.58	78	1014
78157—Bolshoi Arkadak river	1.5	142	-	0.12	73	1314
76646—Anzirka river	2.5	182	0.80	1.55	56	226
77222—Birla river	1.2	189	0.15	0.95	58	106

2.2. Data

The following spatial data on natural and anthropogenic factors were used as input for WATEM/SEDEM: topography (as a DEM), map of land use/land cover types (with the spatial distribution of arable lands, forests, meadows, rivers, anthropogenic objects), and soil erodibility. The rainfall erosivity factor is set to be constant.

The spatial data of natural–anthropogenic factors used to implement the SEA/Balance methodology are similar: relief (in the form of maps of slope angles, aspect, plane and profile curvature, directions of surface slope runoff), map of land use, and soil erodibility. Additionally, the maps of rainfall erosivity factor and snow water storage were provided for SEA/Balance input. The data used to prepare the spatial models for calculating the erosion–accumulative sediment balance are described below.

2.2.1. Relief and LS-Factor

The maps with morphometric characteristics (slope angle, aspect, profile, and plan curvature), flow directions, and catchment boundaries were obtained using the global publicly available SRTM SIR-C elevation model [36] with 1 angular second resolution, which is close to 25×25 m cell size grid of the study area (<https://lta.cr.usgs.gov/>, accessed on 25 July 2021). This model also provides more accurate morphometric elevation characteristics required for calculating soil erosion losses than other global open source DEMs with similar resolution [37,38]. The hydrological correction of the relief model was performed to remove local depressions for further calculation of the LS-factor [39,40]. The erosion potential of the relief (LS-factor) is estimated in different ways in the used methods. The approach described in the article of Desmet and Govers [41] is used to assess the LS-factor in the WATEM/SEDEM methodology. The SEA/Balance methodology uses the Formula (1) to evaluate the LS-factor:

$$LS = 22.1^{-p} L^p \frac{18.62 \sin \left[\arctg \left(\frac{1}{100} I \right) \right]}{1 + 10^{0.339 - 0.06I}} + 0.065 \quad (1)$$

where I is the slope (%), L is the slope length (m), and p is determined by Equation (2), as follows:

$$p = 0.2 + 2.352(p_0 - 0.2)L^{-0.15} \quad (2)$$

where p_0 —slope percent < 1% is 0.2, 1–3% is 0.3, 3–5% is 0.4 and >5% is 0.5.

2.2.2. Field Observations

Suspended sediment yield (SSY) data at stationary gauging stations were used to verify the modeling results. The database on water and sediment yield for the study area was formed earlier [42] based on measurements of water turbidity, which were obtained at the posts of the state monitoring network of Russia. These turbidity values were obtained in manual mode using ashless medium (11 cm Ø) filters with a pore size of 8–12 microns. Observations of water turbidity in most of the studied river basins, based on which sediment yield is calculated, were carried out with a frequency of 3 times a day. However, we only had annual average data. The years of observation for SSY and the duration of the observation series for each gauging station are presented in Table 3.

Table 3. Years of observation of suspended sediment yield.

River Basin ID	River	Observation Period	Duration (Years)
77194	Betka	1946, 1963–1975	14
76644	Nurminka	1963–1985	22
77217	Malyy Cheremshan	1963–1980	18
76324	Sterlya	1986–1989, 1992–2013	35
76522	Menzelia	1963–1981	18
76520	Mellya	1964–1981	18
75647	Rudnya	1967–1984	15
78205	Atkarka	1965–1975	11
78157	Bolshoi Arkadak	1963–1975	13
76646	Anzirka	1965–1975	11
77222	Birla	1967–1982	11

2.2.3. Land Use

The spatial models of land use were created based on Landsat data. The initial Landsat data for the study area have a grid size of 1 angular second. Land use dynamics

were estimated based on Landsat 5 data for the period 1985–1990, and Landsat 8 data for 2013–2015. Cloudless multiseasonal images for the snow-free period were used for this purpose. The chosen years of imagery were determined by the fact that most of the gauging stations used for measurements of suspended sediment yield and that were used for further verification of modeling results have an observation period from the 1960s to 1980s (Table 3). The use of images from earlier satellites (Landsat 4 MSS) is not reasonable because of their lower quality and spatial resolution. It is also accepted that the land use of the study area during this period (the 1960s to 1980s) was relatively constant [43]. However, according to earlier research, there have been some changes in land use patterns in the study area over the past 30 years (1985–1990 to the present). They are associated with decreased cropland area use and their abandonment [44].

The analysis of multi-temporal images within the Sterlya river basin showed negligible dynamics in land use from 1985–2015. There is a 6% decrease in arable land area in this river basin and a 4.4% increase in grassland area (Table 4).

Table 4. Dynamics of land use within the test River Basin 76324 (Sterlya river basin).

Land Category	1985–1990		2013–2015	
	Area, ha	Percent of the Total Area	Area, ha	Percent of the Total Area
Water bodies	39	0.06	35.1	0.06
Forests	4584.18	7.75	4602.6	7.79
Meadows	16,373.18	27.69	18,966.15	32.08
Cropland	36,571.01	61.88	32,924.00	55.67
Urban areas	1548.63	2.62	2588.15	4.4
Total	59,116	100	59,116	100

Composites were created for land use recognition, based on bands 1–5 and 7 for Landsat 5, and bands 2–6 for Landsat 8, calculated NDVI indices, and statistical metrics (mean, median, max, sum, STD) calculated from NDVI. Recognition was performed using the Random Forest method. A training sample was prepared, including five land-use types to train the classifier within each river basin: croplands, forests, meadows, water bodies, and urban objects (significant roads, settlements). As a result of the classification, a map of land use was obtained for each river basin. Separately, it is worth mentioning that small rivers are not visible on Landsat images due to their resolution, so the layer of water objects digitized from topographic maps of scale 1:100,000 was used additionally. This layer is required to assess the correctness of the methodology, which is based on the assessment of the average annual intensity of sediment outflow into rivers.

Based on the obtained land use map and the map of landscape zones, different values of the C (crop management factor) factor were established for different categories of land use. For arable land, these values were taken from the article [45] based on information from the Russian State Committee on Statistics of typical crop rotations in each landscape zone (<http://www.gks.ru>, accessed on 25 July 2021).

Because there is no free available spatial information about how to cultivate land over such a large territory, P—the erosion control practice factor, was assumed to be 1.

2.2.4. Precipitation

The model of rainfall erosivity factor for both models (WATEM/SEDEM and SEA/BALANCE) was created based on Equation (3) proposed for the Middle Volga region [46] for each test river basin.

$$R = 3.19e^{0.006P} \quad (3)$$

where R —rainfall erosivity factor ($t \text{ m mm ha}^{-1} \text{ min}^{-1} \text{ year}^{-1}$), and P —the long-term average annual sum of the daily rainfall depth over 10 mm during the warm season. The

units of measurement were converted to the SI measurement system to use the values of R obtained by Equation (3) in the WATEM/SEDEM model.

The complete methodology for creating a raster model (map) of the rainfall erosivity factor is presented in detail in the article [47]. It should be noted that the initial data on the daily precipitation has been downloaded from RIHMI-WDC (<http://meteo.ru/>, accessed on 10 July 2021) for the corresponding time interval of sediment yield measurement.

A raster map of snow water storage was created based on G.A. Larionov's map [48]. This map shows the thickness of the water layer (mm) that will cover this study area after the melting of snow accumulated over the winter. Data on snow water storage are up to date as of the 1980s. They correspond to the temporal period of observational data of the suspended sediment yield at gauging stations.

Since one of the goals of this work is to evaluate the dynamics of sediment yield within a catchment, the dynamics of the amount of precipitation within that river basin are given here (Table 5). It should be noted that, for the warm period, only precipitation with an intensity of more than 10 mm per day was considered, since this value is most often taken as the threshold from which soil erosion begins during rain events precipitation [3].

Table 5. Effective precipitation (>10 mm/day) dynamics in the Sterlya river basin.

	Cold Period 1986–1990 (mm)	Warm Period 1986–1990 (mm)	Cold Period 1991–2013 (mm)	Warm Period 1991–2013 (mm)
st. Sterlitamak—Sterlya River	222	156	216	173

The analysis of the table shows that the amount of precipitation with an intensity of more than 10 mm/day in the warm period of the year at the studied station increased by 11%. The amount of precipitation falling out in the cold period of the year decreased by 5%.

2.2.5. Soils

Raster maps of soil erodibility (K-factor) were prepared based on the data of the Unified State Register of Soil Resources of Russia (USRSR) (<http://egrpr.esoil.ru>, accessed on 10 July 2021) using Equation (4).

$$K = \left[16.67 \times \{d \times (100 - e)\}^{1.14} \times (10^{-6}) \times (12 - a) + 0.25 \times (b - 2) + 0.193 \times (4 - c) \right] \quad (4)$$

where K is soil erodibility factor (t ha min/((t m) ha mm), d is the fraction content of particles 0.1–0.001 mm in size (%), e is the fraction content of particles <0.001 mm in size (%), a is the organic matter (%), b is the classes for structure, and c is the classes for permeability. Units have been converted to SI to use the K values in the WATEM/SEDEM model.

The initial soil map is a vector layer. Polygonal objects of the layer are digitized contours of the Russian soil map at a scale of 1:2,500,000 [49] and contain information on soil types. The selected soil map has a finer spatial scale than the other spatial data used in the study. At the same time, it is currently the only qualitative open-source digital information on soil resources covering the entire study area. In addition, for 6 test river basins (77194—Betka river, 76644—Nurminka river, 77217—Malyy Cheremshan, 76522—Menzelia river, 76520—Mellya river, 76646—Anzirka river) located within one of the subjects of the Russian Federation (Republic of Tatarstan), a more detailed soil map of scale 1:200,000 was available, which was used as an alternative for calculations. Calculations were made using both maps within the given 6 river basins.

2.3. Methodology

The sediment redistribution in river basins was evaluated using the WATEM/SEDEM model and the SEA/Balance model proposed in the current study. The model prediction was compared with the suspended sediment yield monitoring data.

River basins for test calculations and subsequent analysis of methodology accuracy were selected according to the following criteria.

The river basin should have a relatively long observation series (more than ten years) that is necessary to ensure the statistical reliability of stationary observation data.

The catchment should have a large plowed area (>50%), which is necessary for dominance of the contribution of the basin erosion over channel erosion to the observed suspended sediment yield and the possibility of comparison with model prediction [50]. Thus, the contribution of channel erosion to suspended sediment yield is no more than 5–20% within the territory under consideration on heavily plowed river basins (>50%) [51].

The river basin should have a small area of the subcatchment controlled by ponds and reservoirs (25% on average for the whole river basins) to minimize the influence of hydraulic structures (ponds, reservoirs) on the amount of suspended sediment yield.

The catchments should be small (100–1500 km²). The average long-term maximum water discharges increase with a river basin area rise. This leads to an increase in bank erosion in the study area, as well as to an increase in the channel erosion contribution to suspended sediment yield [51].

2.3.1. WATEM/SEDEM Model

This model is used by various researchers worldwide, and it is described in detail by its developers [34]. WATEM/SEDEM is a methodology based on a raster model of spatial data. In the first stage, the mean annual soil erosion E in the cells of the raster model is calculated using the RUSLE [15] by Equation (5).

$$E = R \times K \times LS_{2D} \times C \times P \quad (5)$$

where E —is the mean annual soil loss (kg m⁻² year⁻¹), R —is the rainfall erosivity factor (MJ mm m⁻² h⁻¹ year⁻¹), K —is the soil erodibility (kg hour MJ⁻¹ mm⁻¹), LS_{2D} —is the slope length and steepness factor (dimensionless), C —is the crop management factor (dimensionless), P —is the erosion control practice factor.

In the second stage, the transport of eroded material is simulated. Sediment movement is estimated until the river element is reached. The sediment transport is calculated using transport capacity (Equation (6)):

$$TC = ktc \times R \times K \times (LS_{2D} - 4.1 \times S_{IR}), \quad (6)$$

where TC is the transport capacity (kg m⁻² year⁻¹), ktc —is the transport capacity coefficient (m) depending on the type of land cover, S_{IR} —is the interrill slope gradient factor, and the other variables are the same as in Equation (5).

The amount of sediment delivered from the up-slope areas is added to sediment produced by erosion (E) for each grid cell. If the sum exceeds the transport capacity (TC) of the flow, then the sediment yield from the cell is limited to the transport capacity. If the sum of the sediment delivered to a given grid cell and the sediment formed by erosion in that cell is lower than the transport capacity of the flow, then all the sediment is transported further down the slope.

The model can be run by the original software tool downloaded from the Catholic University of Leuven's official website. The model uses two values of ktc : ktc_{high} —for arable land; ktc_{low} —for unploughed land. We used the values of the coefficients by default set in the software package when modeling within the studied river basins: $ktc_{high} = 250$ and $ktc_{low} = 75$. The calculation of the model was performed on a grid with a cell size of 25 × 25 m.

2.3.2. SEA/Balance Model

The following Equation (7) was taken as the basis to calculate the sediment budget on the river basins slopes by SEA/Balance model [50,52]:

$$\Delta W = (W_{se} + W_{re}) - W_a \quad (7)$$

where ΔW —a mass balance between erosion and accumulation (t/year), W_{se} —a mass of sheet erosion (t/year), W_{re} —a mass of raindrop erosion (t/year), and W_a —a mass of accumulation (t/year). The raster model of spatial data used in this study is based on a grid with a cell size of 25×25 m.

Equation (7) can be rewritten by replacing $(W_{se} + W_{re})$ with $W_{j,in}$, and W_a with $W_{j,out}$, and by adding $W_{i,in}$ (Figure 2, Equation (8))—the sediment that comes from the cells located higher on the slope:

$$W_j = \left(\sum_{i=1}^n W_{i,in} \right) + W_{j,in} - W_{j,out} \tag{8}$$

where W_j is the budget of mean annual intensity between soil erosion/accumulation in the current j -th grid cell(t/year), n is the number of cells located up the slope from which sediment is coming, $W_{i,in}$ is the mean annual intensity of sediment yield coming into the current cell from the i -th cell located up the slope (t/year), $W_{j,in}$ is the mean annual intensity of sediment generation in that cell (equal to the erosion losses of the soil in that cell calculated by Equation (9) (t/year)), and $W_{j,out}$ is the mean annual intensity of the sediment accumulation in the cell (t/year).

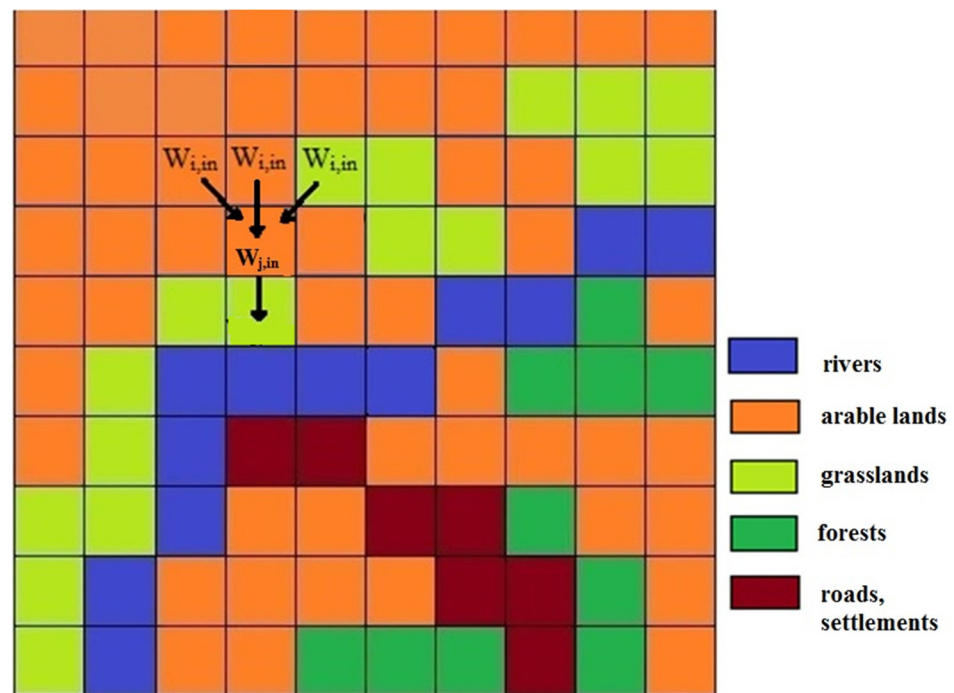


Figure 2. Schematic diagram of sediment balance assessment in a specific cell of the raster.

The total amount of sediment in a cell was estimated similarly to the WATEM/SEDEM model [34], but instead of RUSLE, the method proposed by Moscow State University (MSU) was used [40]. The amount of sediment delivered from other cells is added to the sediment generated during soil erosion. Another difference between SEA/Balance model and from WATEM/SEDEM model is the method of a quantitative assessment of the sediment yield from the raster cell. While the WATEM/SEDEM methodology uses the transport capacity characteristic to estimate the sediment transported from the cell and the sediment that remains in the grid cell, the sediment delivery ratio (SDR) is used in SEA/Balance model. We take the SDR as the fraction of sediment transported from a given grid cell to a cell downstream.

The intensity of sediment generation in the cell itself is calculated by Equation (9).

$$W_{j,in} = E_j A_j \tag{9}$$

where E_j —is the soil loss from rainwater and snowmelt runoff (t/ha per year), calculated by the Formula (10) [7,48], and A_j —area of each grid cell (ha).

$$E_j = E_{rain} + E_{snow_melt} \tag{10}$$

where E_{snow_melt} is the annual snowmelt soil erosion (t/ha per year), and E_{rain} is the annual intensity of soil erosion from rainwater. A more detailed description of the calculation of E_{snow_melt} and E_{rain} is given in the article [7].

If we accept that the sediment yield into the cell down the slope will be equal to $SDR_j \times ((\sum_{i=1}^n W_{i,in}) + W_{j,in})$, then Equation (8) can be rewritten in the following form:

$$W_j = ((\sum_{i=1}^n W_{i,in}) + W_{j,in}) * (1 - SDR_j) \tag{11}$$

where SDR_j is the sediment delivery ratio for each grid cell.

Previously published field data from arable slopes in the EPR were used to determine averaged SDR for slopes of various configurations. The quantitative ratios of the eroded and accumulated material volumes inside the arable land were determined by three field methods: soil truncation method [53–58], ¹³⁷Cs technique [58–67], and direct measurements of erosion and deposition forms after erosion events [2,68]. Each of these methods characterize the features of sediment redistribution for different time intervals of the entire period of agricultural development. SDR estimates obtained based on each method were aggregated into 8 groups based on slope morphology (Table 6), namely convergent and divergent slopes of planned curvature, convex and concave profile curvature of slopes, and divided into flatter (<3°) and steeper ≥ 3°). Since the assessments were carried out only for arable slopes of plain areas, where, in general, the slopes of arable land are small [58,64,69], the used division of slopes by average steepness seems to be justified. Based on the values of sediment delivery ratios obtained for each type of slope, the average SDR was obtained, which was used in calculations using the SEA/Balance model (Table 6). The obtained average values of the SDR for different types of slopes are comparable with the SDR for slopes of a similar configuration, identified for other regions of the world [70–74].

Table 6. Sediment delivery ratio used in calculations of sediment redistribution in arable land.

		Plan Curvature			
		+(Concave, Convergent)		–(Convex, Divergent)	
Profile Curvature	+(concave)	Slope angle ≥ 3°	Slope angle < 3°	Slope angle ≥ 3°	Slope angle < 3°
		0.71	0.31	0.71	0.31
	–(convex)	Slope angle ≥ 3°	Slope angle < 3°	Slope angle ≥ 3°	Slope angle < 3°
		0.78	0.59	0.86	0.32

We do not consider a budget of sediment yield within the boundaries of major roads and settlements since these territories occupy from 0.2% (the Birla River) to 4.4% (the Sterlya River) of the total catchment area in this study. Therefore, the SDR for territories with settlements and roads was assumed to be 0.

Many publications [40,56] on the spatial distribution of eroded material within forest-covered areas of the Russian Plain show an almost complete absence of surface runoff. Therefore, within the framework of this methodology, the SDR for forest-covered areas was also assumed to be equal to zero.

Eroded material is often transported into the river valley and then into the river through the gully and dry valley network channels. Sediments pass through gullies in transit, or most of them are redeposited on the grassed bottoms of the dry valley. It should be noted that the proportion of territories covered by gullies, which are characterized by a

high SDR, is currently insignificant in the plain part of the European part of Russia [65]. In addition, the spatial detail of the study is a technical limitation in considering the gully network in the delivery of sediments. Landsat imagery with a 30 m spatial resolution corresponds to the detail of our study. These images showed that land-use types are detected quite reliably. Given that the average length of gullies on this territory is 64 m [75], it is impossible to detect most gullies on Landsat images. In addition, an analysis of the development of gullies in various parts of the Russian Plain reveals a clear tendency towards a decrease in the growth rate of both primary and secondary gullies in the second half of the 20th century [76]. Therefore, in this study, we did not consider the gullies as channels for the delivery of sediments to rivers.

The dry valley network was not identified directly on the land-use map. However, it was interpreted in the combined analysis of the morphometric factor maps (convergent plane curvature and large values of the flow length) and the land use map (presence of meadows). Areas satisfying such conditions were assigned the SDR value of 0.15. This value was taken based on averaging data on sediment accumulation in the bottoms of dry valleys, mainly located within the southern megaslope of the Russian Plain. So, for example, for the river Khoper, this indicator varies from 0.45 for first-order valleys to 0.1 for the fifth-order valleys. Moreover, if we take into account here the length of these valleys or their area, then the sediment delivery ratio will be equal to 0.12 to 0.16 [61]. Only sporadic studies have been conducted within the study area that would allow a discussion of the value of the SDR of the bottoms of the gullies of different orders. For example, in 2018–2019, a study was conducted within Temeva Rechka (Mesha River) that showed a sediment delivery factor of 0.20 for a dry valley [77]. Two coefficients were adopted for meadow slopes between cropland and the valley network in this study: 0.15 for concave areas that concentrate flow; 0 for convex areas that disperse the flow.

2.3.3. Comparative Analysis Method

Two features of WATEM/SEDEM and SEA/Balance predictions were compared. First, the accuracy of the two methods was quantitatively compared, expressed as the bias between predicted sediment yield discharged into the river and the observed mean annual suspended sediment yield. Secondly, a qualitative comparative analysis of the net erosion maps was undertaken.

The modeled value sediment mass entering the river channel from the river basin and the measured sediment at some sections of the river are not the same. For example, the suspended sediment yield (SSY) of a river measured at a particular site can be estimated by Equation (12).

$$W = W_{\text{wsd}} + W_{\text{che}} - W_{\text{accrch}} - W_{\text{accwsd}} \quad (12)$$

where W_{wsd} is the mass of sediment coming from the river basin (t), W_{che} is the mass of sediment produced by channel erosion (t), W_{accrch} is the mass of sediment accumulating in the river channel (t), W_{accwsd} is the mass of sediment accumulating in the river basin (t), and W_{wsd} and W_{accwsd} values are considered in the SEA/Balance methodology. Since sediments of river basin origin within heavily plowed catchments to a greater extent form the suspended sediments yield, determining the turbidity of water, the sediments of channel genesis are mainly transported along the bed in the form of sand and gravel [78]. It can be assumed that the W_{che} value will give a relatively small contribution to the SSY measured in the river channel. This statement is confirmed by the fact that we are studying heavily plowed (more than 50%) river basins, where, according to previous studies [51], the share of the channel part of SSY is in the range of 5–20%. The value of W_{accrch} can also be ignored because according to the published data, the process of active silting of small rivers was substantially slowed down and the share of channel accumulation in the total mass of sediment yield is small in the second half of the 20th century [79].

The evaluation methodology's accuracy consisted of a comparative analysis of the biases between modeled sediment yield (SSY_{mod}) coming from the territory of the river

basin with the observed values (SSY_{obs}) of the suspended sediment yield in the river channel. The proposed estimation approach is standard and tested in many studies [9,33].

The bias (ERR) between the observed and simulated SSY values was calculated in a percentage using the Equation (13).

$$ERR = \left(\frac{SSY_{mod} - SSY_{obs}}{SSY_{obs}} \right) * 100 \quad (13)$$

3. Results

Sediment yield values for 11 river basins in various landscape zones of the study area were calculated using WATEM/SEDEM and proposed SEA/Balance models. The biases between their values and the observed sediment yield are presented in Table 7.

Table 7. Results of modeling and comparison with observed data on sediment yield.

River Basin ID	River	SSY_{mod1}^* (t/km ² per Year)	SSY_{mod2}^* (t/km ² per Year)	SSY_{obs}^* (t/km ² per Year)	ERR_{mod1}^* , %	ERR_{mod2}^* , %
77194	Betka	323	341	365	−12	−7
76644	Nurminka	115	410	246	−53	+67
77217	Malyy Cheremshan	37	67	84	−56	−21
76324	Sterlya	16	42	33	−51	+28
76522	Menzelia	223	186	264	−15	−30
76520	Mellya	77	65	55	+41	+19
75647	Rudnya	92	112	69	+33	+62
78205	Atkarka	11	18	36	−70	−51
78157	Bolshoi Arkadak	31	37	34	−8	+9
76646	Anzirka	81	163	363	−78	−55
77222	Birla	3	12	6	−53	+96

Note(s): * SSY_{mod1} —the modeled suspended sediment yield (SEA/Balance methodology). SSY_{mod2} —the modeled suspended sediment yield (WATEM/SEDEM). SSY_{obs} —the observed suspended sediment yield. ERR_{mod1} —the bias between modeled (SEA/Balance) and observed suspended sediment yield. ERR_{mod2} —the bias between modeled (WATEM/SEDEM) and observed suspended sediment yield.

The absolute average bias (ERR_{mod1}) between modeled and observed suspended sediment yield in the SEA/Balance methodology is 43%. The WATEM/SEDEM methodology's bias (ERR_{mod2}) is slightly lower—40%. In addition, a bias analysis was carried out separately in each river basin, which made it possible to split 11 test river basins into three groups (Table 7). In the first group (six river basins), the absolute biases are smaller in the case of using the WATEM/SEDEM (Betka, Malyy Cheremshan, Sterlya, Mellya, Atkarka, Anzirka) methodology. The second group (four river basins) with the smallest absolute biases are in the case of using the SEA/Balance method (Nurminka, Menzelia, Rudnya, Birla). The third group includes the basin of the Bolshoi Arkadak river, which is characterized by almost the same absolute biases.

However, suppose the trend (sign “+” or “−”) of bias is considered in the calculations. In that case, the biases in measured and calculated values using the are +11%, and −29% using the WATEM/SEDEM and SEA/Balance methodologies, respectively. Partly negative bias (−29%) can be explained by the contribution of channel erosion, which, for these heavily plowed basins, can reach 5–20% [51].

The positive bias (+11%) associated with using the WATEM/SEDEM methodology is difficult to explain because the sediment yield from the catchment must be less than the suspended sediment yield measured in the river since in the river the contribution

of channel erosion is added to basin erosion. The analysis of all 11 river basins (Table 7) shows that the values of suspended sediment yield obtained within 9 river basins by the SEA/Balance method have negative biases, and only 2 (Mellia, Rudnya) have positive values. The number of river basins with positive and negative values of biases using the WATEM/SEDEM methodology is almost equal.

It is noteworthy that, for some test river basins (Nurminka, Sterlya, Birla), very different values of sediment yield were obtained using two different models. This can be explained by the fact that the WATEM/SEDEM model was not calibrated for the natural conditions of Russia due to insufficient initial data. Therefore, we have positive biases values here within these river basins (Nurminka, Sterlya, Birla) in the case of application of WATEM/SEDEM model calculation.

Estimating errors of both models for six test river basins (Betka River, Nurminka River, Malyy Cheremshan River, Menzelia River, Melya River, Anzirka River) does not significantly change the result in the case of using in the calculation the a more detailed information about soil parameters taken from soil map (scale 1:200,000).

Determination coefficients of linear models relating the observed and predicted data by SEA/Balance methodology and WATEM/SEDEM model are as follows: SEA/Balance— $R^2 = 0.6$; WATEM/SEDEM— $R^2 = 0.63$, which demonstrates a rather high correlation between observed and model values obtained by two different methods. Thus, correlation coefficients between the observed values and the predicted values obtained using both methods are around 0.8 (0.78—SEA/Balance, 0.79—WATEM/SEDEM). These correlation coefficients are characterized by p-values less than 0.05, which indicates a statistically significant non-zero correlation between the two variables. The obtained results of the correlation analysis are illustrated by the graphs of linear models between the observed and simulated SSY values (Figures 3 and 4).

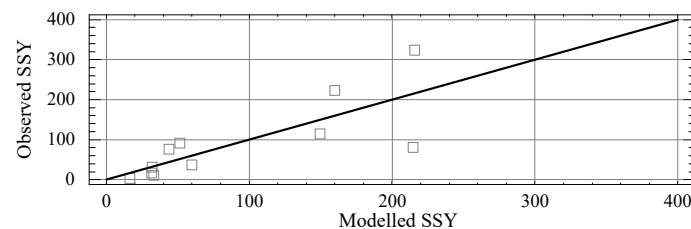


Figure 3. Plot of linear model between observed SSY_{obs} (t/km^2) and modeled SSY_{mod1} SEA/Balance (t/km^2) ($SSY_{obs} = 13.3072 + 0.55474 * SSY_{mod1}$).

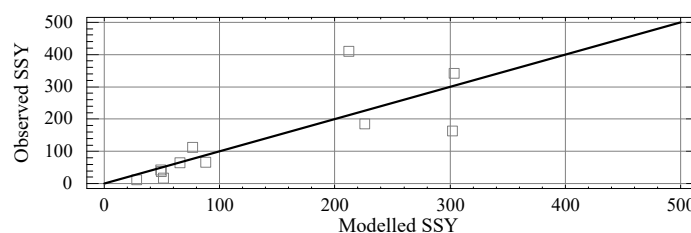


Figure 4. Plot of linear model between observed SSY_{obs} (t/km^2) and modeled SSY_{mod2} WATEM/SEDEM (t/km^2) ($SSY_{obs} = 31.4649 + 0.831994 * SSY_{mod2}$).

The maps of the mean annual net water erosion are an actual result of the study. The majority of similar studies usually present only maps of sediment yield from a given area. A cartographic representation of the net water erosion in the various parts of the EPR is reported much more rarely.

Map analysis shows that (Figures 5 and 6) soil loss intensity values obtained by the SEA/Balance model are less than the values obtained by the WATEM/SEDEM model in the same areas. At the same time, both methods systematically show that the highest values of soil loss intensity are associated with steep sections of slopes (Figures 5 and 6).

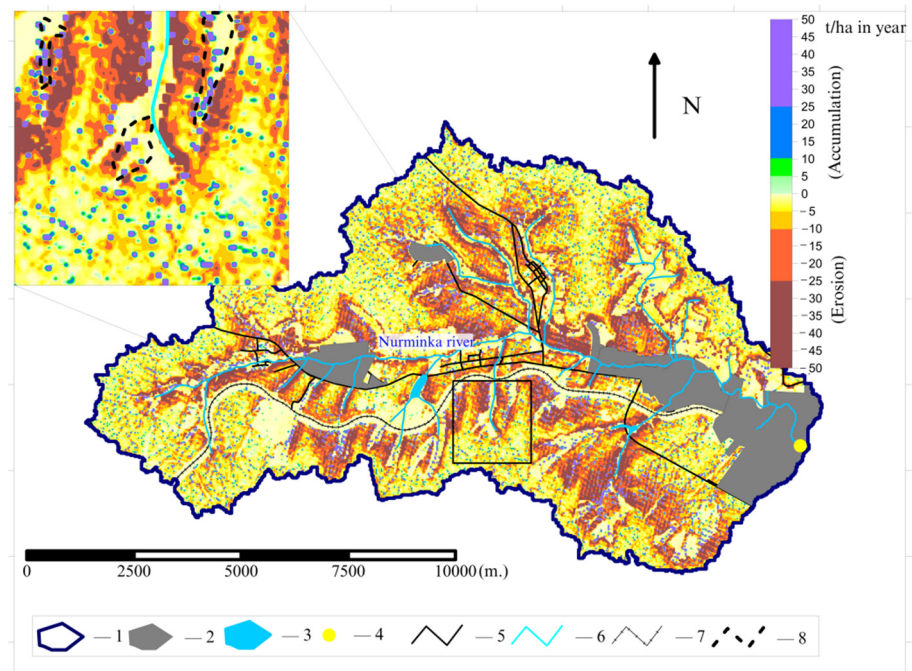


Figure 5. Map of the net water erosion obtained using WATEM/SEDEM methodology for Nurminka river basin (Numbers: 1—river basin boundary, 2—settlements, 3—water bodies, 4—SSY observation station, 5—roads, 6—rivers, 7—railroads, 8—sediment accumulation places within dry valleys and terrace joints).

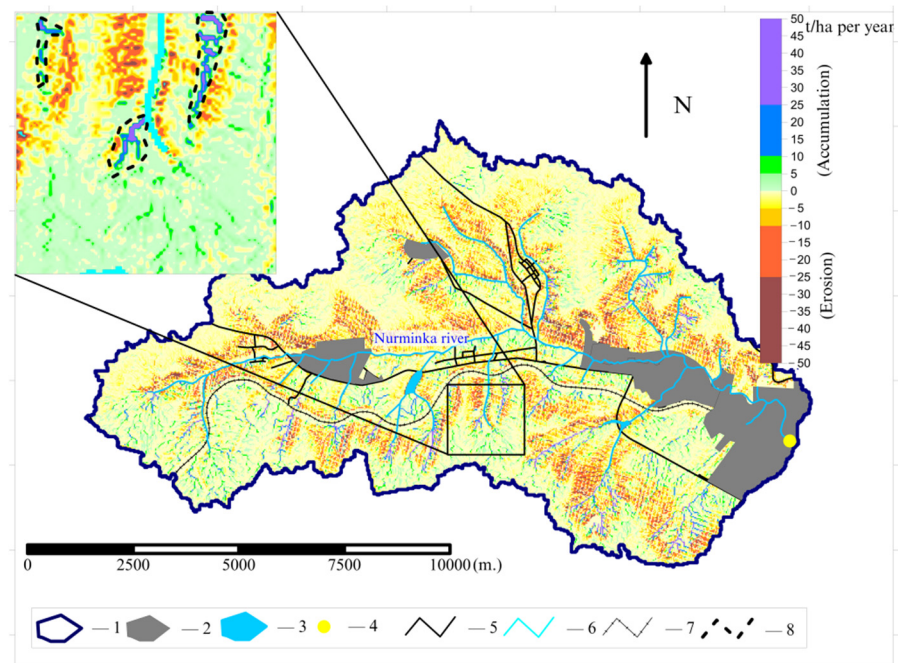


Figure 6. Map of the net water erosion obtained using SEA/Balance methodology for Nurminka river basin (Numbers: 1—river basin boundary, 2—settlements, 3—water bodies, 4—SSY observation station, 5—roads, 6—rivers, 7—railroads, 8—sediment accumulation places within dry valleys and terrace joints).

The spatial distribution of intensities of accumulation differs between SEA/Balance and WATEM/SEDEM models. So, on the map obtained by the SEA/Balance technique, the most significant accumulation is related to the dry valley network and the terrace joints

of the steep slopes. On the map obtained by the WATEM/SEDEM technique, the pattern of the most significant accumulation refers to the bottoms of the dry valleys and occupies a smaller area. The spatial distribution of erosion and accumulation zones predicted by models requires to be verified by field studies which could also give a quantitative assessment of the intensity of the processes.

The possibility of applying the proposed SEA/Balance methodology to other parts of European Russia can be assessed after carrying out similar test analyses and comparing them with stationary observation data.

Analysis of Sediment Yield Dynamics

Land use and precipitation are the two most significant factors affecting the intensity of the erosion–accumulation processes and sediment yield for the last 30 years within the study area [3]. The modeled dynamics of sediment yield were analyzed within the Sterlya river (76,324) basin, depending on land use change and precipitation since we had relatively modern observed data on sediment yield. The analysis was performed using the SEA/Balance methodology.

As noted above, there has been a reduction in arable land and changes in their spatial position within the Sterlya river (76324) basin. These changes reduced the slope angle and length of the slope in the arable land (Table 1), which led to a 19% reduction in the mass of sediment from the river basin into the river (Table 8).

Table 8. Changes of sediment yield reaching the Sterlya River from the basin modeled by SEA/Balance, depend on changes in precipitation intensity and land use.

Factors that Changed in the Calculation for the Two Periods	1985–1990 (t/y)	1991–2013 (t/y)	Change, %
Change in land use	9219	7502	−19
Change in precipitation	9219	10,098	+10
Change in land use and precipitation	9219	8232	−11

Multidirectional changes in the amount of rainstorm and snowmelt precipitation resulted in an increase in sediment mass reaching the river by 10% in the simulation (Table 8). The simultaneous consideration of changes in both factors leads to an 11% decrease in the sediment mass reaching the river from the catchment from 9219 t/year to 8232 t/year, which corresponds to the dynamics of changes in SSY at the gauging station. At the same time, the dynamics of the SSY values measured at the gauging station are much more significant and change from 68 t/km²/year in 1986–1990 to 25 t/km²/year in 1991–2013. The decrease is 63% of the initial value.

This circumstance is explained by the fact that, since the early 1990s, winters in the study area have become much warmer. The mean annual air temperatures of the winter months have increased, and the depth of soil freezing has decreased [80]. This fact led to a rapid reduction in melted surface runoff [81] and reduced sediment mobilization [3]. Although the SEA/Balance methodology has been used to estimate soil loss from melt runoff, its share in the average annual values of soil erosion, according to the calculation methodology used, does not exceed 10%. In reality, according to the field observations, the contribution of melt runoff to soil erosion at the end of the 1980s was 40% of the total soil losses [82]. It is close to 0% according to modern studies [83,84]. Therefore, the model does not reflect the significant decrease in sediment yield observed at the gauging station. The main difference between meltwater runoff and stormwater runoff is the redistribution of sediments outside the arable land. When meltwater runoff is formed, the turbidity of water is not high. It rarely reaches 100 g/L, but the runoff rates are high, eventually delivering a significant portion of the sediment to permanent streams [61]. In contrast, with storm runoff, the turbidity of the water is often relatively high, leading to the redeposition of most of the sediment along the border of the arable land [68] and in the dry valleys' bottoms, and only a tiny proportion of the sediment is transported to the permanent streams.

4. Discussion

The model bias for SEA/Balance is 43% and WATEM/SEDEM is 40%, which is comparable to the results of similar studies in Belgium [34], where the bias between the model and observed values was 36%.

The obtained coefficients of determination are comparable with the data of another study for the territory located within the Loess Plateau in China [24]. Thus, the R^2 for the linear correlation between the observed and model data of the suspended sediment yield in the Loess Plateau area is 0.69.

WATEM/SEDEM model studies conducted within Spain in 68 river basins [9] show slightly worse results ($R^2 = 0.48$) compared to the modeling of 11 river basins in the European part of Russia. Applying the WATEM/SEDEM model to 40 Italian river basins [31] gives $R^2 = 0.5$ and a mean error of 14%.

It is necessary to consider the fact that the observed data on suspended sediment yield is measured with error. For example, in Belgium, according to estimates [34], the error of suspended sediments yield measurement at gauging stations is 20%. An analysis of suspended sediment yield assessment (average 20-year series) within France shows that the median deviation is 15% [85]. There are data on measurement accuracy at the stations of the state monitoring network of Russia, which we used to assess the bias of the two methods. The accuracy of water turbidity measurements may vary from 10 to 60%, according to methodological guidelines [84].

Thus, we can say that the biases obtained in the current study are comparable with the data of previous studies and do not exceed the errors of field measurements.

5. Conclusions

A comparative analysis of 11 test river basins within the eastern Russian Plain showed that the absolute average bias calculated between the predicted and observed values of SSY is 40% for the WATEM/SEDEM model and 43% for the SEA/Balance model, which, in our opinion, are comparable values. The average bias between measured and predicted values using the WATEM/SEDEM approach is +11%. Average bias for the SEA/Balance approach −29%, which can be presumably explained by the contribution of channel erosion to the observed values.

The sediment yield values obtained by both methods have high correlation coefficients with the observed SSY values within 11 tested river basins: SEA/Balance— $r = 0.78$, WATEM/SEDEM— $r = 0.79$. The methods tested in the article have the following determination coefficients: SEA/Balance— $R^2 = 0.6\%$; WATEM/SEDEM— $R^2 = 0.63\%$.

The methods slightly differ in analyzing the spatial distribution of the deposition sites. So, we cannot see intensive deposition in the lower parts of dry valleys within the test basins calculated by the WATEM/SEDEM model, in contrast to the SEA/Balance model. Here, additional field studies are required within the river basins in question to assess the correctness of spatial distribution on the water erosion maps obtained by both methods.

It is possible to obtain more realistic values of sediment yield delivered from the catchment to the river channels received by using the SEA/Balance model, in comparison with WATEM/SEDEM model for the studied area. At the same time, the model we propose uses regional values of sediment delivery ratio coefficients, which cannot be applied to other territories without field investigation of sediment redistribution within catchment areas.

The analysis of the dynamics of sediment transported to the Sterlya River from its river basin showed an 11% decrease in sediment mass from 1986 to 2013 using SEA/Balance model. Such dynamics have the same direction of the trend compared with changes in the SSY measured at the gauging station, but the reduction in intensity according to field observations is much higher and amounts to 63%.

Author Contributions: Conceptualization, K.M. and V.G.; methodology, K.M.; software, K.M.; validation, K.M.; formal analysis, O.Y.; investigation, K.M.; resources, M.I. and N.C.; data curation, M.I. and N.C.; writing—original draft preparation, K.M.; writing—review and editing, K.M., V.G. and O.Y.; visualization, K.M.; funding acquisition, O.Y. All authors have read and agreed to the published version of the manuscript.

Funding: The study was carried out with the support of the Russian Science Foundation project 22-17-00025—preparation and analysis of data; the Russian Science Foundation project 21-17-00181 mathematical and statistical data processing; the Kazan Federal University Strategic Academic Leadership Program (“PRIORITY-2030”)—working methodology and software.

Institutional Review Board Statement: Not applicable.

Informed Consent Statement: Not applicable.

Data Availability Statement: Not applicable.

Conflicts of Interest: The authors declare no conflict of interest.

References

1. Walling, D.E. The Sediment Delivery Problem. *J. Hydrol.* **1983**, *65*, 209–237. [[CrossRef](#)]
2. Litvin, L.F. *Geography of Soil Erosion of Agricultural Lands in Russia*; Akademkniga: Moscow, Russia, 2002.
3. Golosov, V.; Yermolaev, O.; Litvin, L.; Chizhikova, N.; Kiryukhina, Z.; Safina, G. Influence of Climate and Land Use Changes on Recent Trends of Soil Erosion Rates within the Russian Plain. *Land Degrad. Dev.* **2018**, *29*, 2658–2667. [[CrossRef](#)]
4. Prishchepov, A.; Müller, D.; Dubinin, M.; Baumann, M.; Radeloff, V.C. Determinants of the Spatial Distribution of Abandoned Agricultural Lands in the European Part of Russia. *Spat. Econ.* **2013**, *3*, 30–62. [[CrossRef](#)]
5. Ivanov, M.A.; Prishchepov, A.V.; Golosov, V.N.; Zalyaliev, R.R.; Efimov, K.V.; Kondrat’eva, A.A.; Kinyashova, A.D.; Ionova, Y.K. Method of Croplands Dynamics Mapping in River Basins of the European Part of Russia for the Period of 1985–2015. *Sovr. Probl. DZZ Kosm.* **2017**, *14*, 161–171. [[CrossRef](#)]
6. Krasilnikov, P.; Makarov, O.; Alyabina, I.; Nachtergaele, F. Assessing Soil Degradation in Northern Eurasia. *Geoderma Reg.* **2016**, *7*, 1–10. [[CrossRef](#)]
7. Maltsev, K.; Yermolaev, O. Assessment of Soil Loss by Water Erosion in Small River Basins in Russia. *Catena* **2020**, *195*, 104726. [[CrossRef](#)]
8. Warren, S.D.; Ruzycki, T.S.; Vaughan, R.; Nissen, P.E. Validation of the Unit Stream Power Erosion and Deposition (USPED) Model at Yakima Training Center, Washington. *Northwest Sci.* **2019**, *92*, 338. [[CrossRef](#)]
9. De Vente, J.; Poesen, J.; Verstraeten, G.; Van Rompaey, A.; Govers, G. Spatially Distributed Modelling of Soil Erosion and Sediment Yield at Regional Scales in Spain. *Glob. Planet. Chang.* **2008**, *60*, 393–415. [[CrossRef](#)]
10. Alatorre, L.C.; Beguería, S.; García-Ruiz, J.M. Regional Scale Modeling of Hillslope Sediment Delivery: A Case Study in the Barasona Reservoir Watershed (Spain) Using WATEM/SEDEM. *J. Hydrol.* **2010**, *391*, 109–123. [[CrossRef](#)]
11. Pietroń, J.; Chalov, S.R.; Chalova, A.S.; Alekseenko, A.V.; Jarsjö, J. Extreme Spatial Variability in Riverine Sediment Load Inputs Due to Soil Loss in Surface Mining Areas of the Lake Baikal Basin. *Catena* **2017**, *152*, 82–93. [[CrossRef](#)]
12. Boardman, J.; Poesen, J. Soil Erosion in Europe: Major Processes, Causes and Consequences. In *Soil Erosion in Europe*; John Wiley & Sons, Ltd.: Chichester, UK, 2006; pp. 477–487, ISBN 978-0-470-85920-9.
13. Borrelli, P.; Alewell, C.; Alvarez, P.; Anache, J.A.A.; Baartman, J.; Ballabio, C.; Bezak, N.; Biddoccu, M.; Cerdà, A.; Chalise, D.; et al. Soil Erosion Modelling: A Global Review and Statistical Analysis. *Sci. Total Environ.* **2021**, *780*, 146494. [[CrossRef](#)]
14. Wischmeier, W.H.; Smith, D.D. *Predicting Rainfall Erosion Losses: A Guide to Conservation Planning*; USDA: Washington, DC, USA, 1978; p. 67.
15. Renard, K.G.; Foster, G.R.; Weesies, G.A.; McCool, D.K. Predicting Soil Erosion by Water: A Guide to Conservation Planning With the Revised Universal Soil Loss Equation (RUSLE). In *Agriculture Handbook*; SSOP: Washington, DC, USA, 1997; ISBN 0-16-048938-5.
16. Dabney, S.M.; Yoder, D.C.; Vieira, D.A.N. The Application of the Revised Universal Soil Loss Equation, Version 2, to Evaluate the Impacts of Alternative Climate Change Scenarios on Runoff and Sediment Yield. *J. Soil Water Conserv.* **2012**, *67*, 343–353. [[CrossRef](#)]
17. Schob, A.; Schmidt, J.; Tenholtern, R. Derivation of Site-Related Measures to Minimise Soil Erosion on the Watershed Scale in the Saxonian Loess Belt Using the Model EROSION 3D. *Catena* **2006**, *68*, 153–160. [[CrossRef](#)]
18. Vigiak, O.; Malagó, A.; Bouraoui, F.; Vanmaercke, M.; Poesen, J. Adapting SWAT Hillslope Erosion Model to Predict Sediment Concentrations and Yields in Large Basins. *Sci. Total Environ.* **2015**, *538*, 855–875. [[CrossRef](#)] [[PubMed](#)]
19. Walling, D.E.; Russell, M.A.; Hodgkinson, R.A.; Zhang, Y. Establishing Sediment Budgets for Two Small Lowland Agricultural Catchments in the UK. *Catena* **2002**, *47*, 323–353. [[CrossRef](#)]
20. Boomer, K.B.; Weller, D.E.; Jordan, T.E. Empirical Models Based on the Universal Soil Loss Equation Fail to Predict Sediment Discharges from Chesapeake Bay Catchments. *J. Environ. Qual.* **2008**, *37*, 79–89. [[CrossRef](#)]

21. Baartman, J.E.M.; Masselink, R.; Keesstra, S.D.; Temme, A.J.A.M. Linking Landscape Morphological Complexity and Sediment Connectivity: Landscape morphological complexity and sediment connectivity. *Earth Surf. Process. Landf.* **2013**, *38*, 1457–1471. [[CrossRef](#)]
22. Heckmann, T.; Cavalli, M.; Cerdan, O.; Foerster, S.; Javaux, M.; Lode, E.; Smetanová, A.; Vericat, D.; Brardinoni, F. Indices of Sediment Connectivity: Opportunities, Challenges and Limitations. *Earth Sci. Rev.* **2018**, *187*, 77–108. [[CrossRef](#)]
23. Borselli, L.; Cassi, P.; Torri, D. Prolegomena to Sediment and Flow Connectivity in the Landscape: A GIS and Field Numerical Assessment. *Catena* **2008**, *75*, 268–277. [[CrossRef](#)]
24. Zhao, G.; Gao, P.; Tian, P.; Sun, W.; Hu, J.; Mu, X. Assessing Sediment Connectivity and Soil Erosion by Water in a Representative Catchment on the Loess Plateau, China. *Catena* **2020**, *185*, 104284. [[CrossRef](#)]
25. Gay, A.; Cerdan, O.; Mardhel, V.; Desmet, M. Application of an Index of Sediment Connectivity in a Lowland Area. *J. Soils Sediments* **2016**, *16*, 280–293. [[CrossRef](#)]
26. López-Vicente, M.; Navas, A.; Gaspar, L.; Machín, J. Advanced Modelling of Runoff and Soil Redistribution for Agricultural Systems: The SERT Model. *Agric. Water Manag.* **2013**, *125*, 1–12. [[CrossRef](#)]
27. Chartin, C.; Evrard, O.; Onda, Y.; Patin, J.; Lefèvre, I.; Ottlé, C.; Ayrault, S.; Lepage, H.; Bonté, P. Tracking the Early Dispersion of Contaminated Sediment along Rivers Draining the Fukushima Radioactive Pollution Plume. *Anthropocene* **2013**, *1*, 23–34. [[CrossRef](#)]
28. Vigiak, O.; Borselli, L.; Newham, L.T.H.; McInnes, J.; Roberts, A.M. Comparison of Conceptual Landscape Metrics to Define Hillslope-Scale Sediment Delivery Ratio. *Geomorphology* **2012**, *138*, 74–88. [[CrossRef](#)]
29. Ferro, V.; Porto, P. Sediment Delivery Distributed (SEDD) Model. *J. Hydrol. Eng.* **2000**, *5*, 411–422. [[CrossRef](#)]
30. Bhattarai, R.; Dutta, D. A Comparative Analysis of Sediment Yield Simulation by Empirical and Process-Oriented Models in Thailand / Une Analyse Comparative de Simulations de l'exportation Sédimentaire En Thaïlande à l'aide de Modèles Empiriques et de Processus. *Hydrol. Sci. J.* **2008**, *53*, 1253–1269. [[CrossRef](#)]
31. Verstraeten, G.; Prosser, I.P.; Fogarty, P. Predicting the Spatial Patterns of Hillslope Sediment Delivery to River Channels in the Murrumbidgee Catchment, Australia. *J. Hydrol.* **2007**, *334*, 440–454. [[CrossRef](#)]
32. Haregeweyn, N.; Poesen, J.; Verstraeten, G.; Govers, G.; de Vente, J.; Nyssen, J.; Deckers, J.; Moeyersons, J. Assessing the performance of a spatially distributed soil erosion and sediment delivery model (watem/sedem) in northern ethiopia: Spatially distributed soil erosion and sedimentation. *Land Degrad. Develop.* **2013**, *24*, 188–204. [[CrossRef](#)]
33. Zhidkin, A.P.; Smirnova, M.A.; Gennadiev, A.N.; Lukin, S.V.; Zazdravnykh, Y.A.; Lozbenov, N.I. Digital Mapping of Soil Associations and Eroded Soils (Prokhorovskii District, Belgorod Oblast). *Eurasian Soil Sci.* **2021**, *54*, 13–24. [[CrossRef](#)]
34. Van Rompaey, A.J.J.; Verstraeten, G.; Van Oost, K.; Govers, G.; Poesen, J. Modelling Mean Annual Sediment Yield Using a Distributed Approach. *Earth Surf. Process. Landf.* **2001**, *26*, 1221–1236. [[CrossRef](#)]
35. *Unified State Register of Soil Resources of Russia, Version 1.0*; Institute of Soil Science: Moscow, Russian, 2014.
36. Farr, T.G.; Rosen, P.A.; Caro, E.; Crippen, R.; Duren, R.; Hensley, S.; Kobrick, M.; Paller, M.; Rodriguez, E.; Roth, L.; et al. The Shuttle Radar Topography Mission. *Rev. Geophys.* **2007**, *45*, RG2004. [[CrossRef](#)]
37. Mal'tsev, K.A.; Golosov, V.N.; Gafurov, A.M. Digital elevation models and their use for assessing soil erosion rates on arable lands. *Uch. Zap. Kazan. Univ. Ser. Estestv. Nauk.* **2018**, *160*, 514–530.
38. Ashatkin, I.A.; Maltsev, K.A.; Gainutdinova, G.F.; Usmanov, B.M.; Gafurov, A.M.; Ganieva, A.F.; Maltseva, T.S.; Gizzatullina, E.R. Analysis of Relief Morphometry by Global DEM in the Southern Part of the European Territory of Russia. *Uch. Zap. Kazan. Univ. Ser. Estestv. Nauki* **2020**, *162*, 612–628. [[CrossRef](#)]
39. Lindsay, J.B. The Terrain Analysis System: A Tool for Hydro-Geomorphologic Applications. *Hydrol. Process.* **2005**, *19*, 1123–1130. [[CrossRef](#)]
40. Lindsay, J.B.; Creed, I.F. Removal of Artifact Depressions from Digital Elevation Models: Towards a Minimum Impact Approach. *Hydrol. Process.* **2005**, *19*, 3113–3126. [[CrossRef](#)]
41. Desmet, J.J.; Govers, G. A GIS Procedure for Automatically Calculating the USLE LS Factor on Topographically Complex Landscape Units. *J. Soil Water Conserv.* **1996**, *51*, 427–433.
42. Yermolaev, O.; Mukharamova, S.; Vedeneeva, E. River Runoff Modeling in the European Territory of Russia. *Catena* **2021**, *203*, 105327. [[CrossRef](#)]
43. Lyuri, D.I.; Goryachkin, S.V.; Karavaeva, N.A.; Denisenko, E.A.; Nefedova, T.G. *Dynamics of Agricultural Lands in Russia in the XX Century and the Postagrogenic Restoration of Vegetation and Soils*; GEOS: Moscow, Russia, 2010; ISBN 978-5-89118-500-5.
44. Ivanov, M.A. Changes of Cropland Area in the River Basins of the European Part of Russia for the Period 1985–2015 Years, as a Factor of Soil Erosion Dynamics. *IOP Conf. Ser. Earth Environ. Sci.* **2018**, *107*, 012010. [[CrossRef](#)]
45. Litvin, L.F.; Kiryukhina, Z.P.; Krasnov, S.F.; Dobrovol'skaya, N.G. Dynamics of Agricultural Soil Erosion in European Russia. *Eurasian Soil Sci.* **2017**, *50*, 1344–1353. [[CrossRef](#)]
46. Kanatieva, N.P.; Krasnov, S.F.; Litvin, L.F. Modern Change of Climate Factors of Erosion in Northern Volga Region. *Soil Eros. Channel Process.* **2010**, *17*, 14–28.
47. Maltsev, K.A.; Yermolaev, O.P. Potential Soil Loss from Erosion on Arable Lands in the European Part of Russia. *Eurasian Soil Sci.* **2019**, *52*, 1588–1597. [[CrossRef](#)]
48. Larionov, G.A. *Eroziya i Deflyatsiya Pochv: Osnovnyye Zakonomernosti i Kolichestvennyye Otsenki (Water and Wind Erosion: Main Features and Quantitative Assessment)*; MSU Publishing House: Moscow, Russia, 1993; ISBN 978-5-211-02467-0.

49. Rukhovich, D.I.; Koroleva, P.V.; Kalinina, N.V.; Vil'chevskaya, E.V.; Simakova, M.S.; Dolinina, E.A.; Rukhovich, S.V. State Soil Map of the Russian Federation: An ArcInfo Version. *Eurasian Soil Sci.* **2013**, *46*, 225–240. [[CrossRef](#)]
50. Alekseevsky, N.I. *Formirovaniye I Dvizheniye Rechnykh Nanosov (Formation and Movement of River Sediments)*; MSU Publishing House: Moscow, Russia, 1998.
51. Dedkov, A. The Relationship between Sediment Yield and Drainage Basin Area. In *Sediment Transfer through the Fluvial System, Proceedings of the Moscow International Symposium, Moscow, Russia, 2–6 August 2004*; IAHS Publication: Wallingford, UK, 2004; Volume 288, pp. 197–204.
52. Dedkov, A.P.; Mozzherin, V.V. *Eroziya i Stok Nanosov na Zemle (Erosion and Sediment Runoff on the Earth)*; Kazan University: Kazan, Russia, 1984.
53. Braude, I.D. *Ratsional'noye Ispol'zovaniye Erodirovannykh Serykh Lesnykh Pochv Nechernozemnoy Zony RSFSR (Rational Use of Eroded Grey Forest Soils in the Non-Chernozem Zone of Russia)*; Lesnaya Promyshlennost Press: Moscow, Russia, 1976.
54. Rozhkov, A.G. O Srednemnogoletney Velichine Smyva Pochv s Pashni v Tsentral'noy Chernozemnoy Zone (About Mean Annual Soil Erosion Rate from Cultivated Field of Central Chernozem Zone). *Nauchno Tekhnicheskiiy Bull. Zacshita Pochv Eroziï* **1977**, *15*, 13–18.
55. Golosov, V.N. Eroziionno-Akkumulyativnyye Protsessy i Balans Nanosov v Basseyne r. Protvy (Erosion-Accumulative Processes and Balance of Sediments in the Protva River Basin). *Bull. Mosc. Univ.* **1988**, *6*, 19–25.
56. Ivanov, V.D.; Nazarenko, N.P. Vliyaniye Eroziionnykh i Akkumulyativnykh Protsessov Na Strukturu Pochvennogo Pokrova Balochnykh Vodoborov (Influence of Erosion and Accumulation Processes on the Structure of the Soil Cover in Dry Valley Catchments). *Eurasian Soil Sci.* **1998**, 1256–1264.
57. Golosov, V.N.; Belyaev, V.R.; Markelov, M.V.; Shamshurina, E.N. Specifics of Sediment Redistribution Within a Small Arable Catchment During Different Periods of Its Cultivation (Gracheva Loschina Catchment, the Kursk Region). *Geomorfologiya* **2015**, *1*, 25–35. [[CrossRef](#)]
58. Zhidkin, A.P.; Golosov, V.N.; Svetlichny, A.A.; Pyatkova, A.V. An Assessment of Load on the Arable Slopes on the Basis of Field Methods and Mathematic Models. *Geomorfologiya* **2015**, *2*, 41–53. [[CrossRef](#)]
59. Golosov, V.N. Redistribution of Sediments on Small River Catchments of Temperate Zone. In *Erosion and Sediment Yield: Global and Regional Perspectives, Proceedings of the Exeter Symposium, Exeter, UK, 15–19 July 1996*; IAHS Publication: Wallingford, UK, 1996; pp. 339–346.
60. Golosov, V.N. Special Considerations for Areas Affected by Chernobyl Fallout. In *Handbook for the Assessment of Soil Erosion and Sedimentation Using Environmental Radionuclides*; Zapata, F., Ed.; Springer: Dordrecht, The Netherlands, 2003; pp. 165–183, ISBN 978-0-306-48054-6.
61. Golosov, V.N. *Eroziionno-Akkumulyativnyye Protsessy v Rechnykh Basseyynakh Osvoyennykh Ravnin (Erosion and Deposition Processes in River Basins of Cultivated Plains)*; GEOS: Moscow, Russia, 2006.
62. Golosov, V.N.; Panin, A.V.; Markelov, M.V. Chernobyl 137Cs Redistribution in the Small Basin of the Lokna River, Central Russia. *Phys. Chem. Earth Part A Solid Earth Geod.* **1999**, *24*, 881–885. [[CrossRef](#)]
63. Panin, A.V.; Walling, D.E.; Golosov, V.N. The Role of Soil Erosion and Fluvial Processes in the Post-Fallout Redistribution of Chernobyl-Derived Caesium-137: A Case Study of the Lapki Catchment, Central Russia. *Geomorphology* **2001**, *40*, 185–204. [[CrossRef](#)]
64. Golosov, V.N.; Ivanova, N.N. Sediment-Associated Chernobyl 137Cs Redistribution in the Small Basins of Central Russia. In *Applied Geomorphology: Theory and Practice*; Allison, R.J., Ed.; John Wiley & Sons: Hoboken, NJ, USA, 2002; pp. 165–181.
65. Bezukhov, D.A.; Golosov, V.N.; Panin, A.V. Evaluation of the Sediment Delivery Ratio of Small Watersheds in the Forest-Steppe and Steppe Regions of the Russian Plain. *Izv. Ross. Akad. Nauk. Seriya Geogr.* **2019**, *4*, 73–84. (In Russian) [[CrossRef](#)]
66. Golosov, V. Application of Chernobyl-Derived 137Cs for the Assessment of Soil Redistribution within a Cultivated Field. *Soil Tillage Res.* **2003**, *69*, 85–98. [[CrossRef](#)]
67. Belyaev, V.; Markelov, M.V.; Golosov, V.; Bonté, P.; Ivanova, N. The Use of Cesium-137 to Assess Modern Agrogenic Transformation of Soil Cover in the Areas Subjected to Chernobyl Fallout. *Eurasian Soil Sci.* **2003**, *36*, 788–802.
68. Belyaev, V.; Golosov, V.; Kislenco, K.S.; Kuznetsova, J.S.; Markelov, M.V. Combining Direct Observations, Modelling, and 137Cs Tracer for Evaluating Individual Event Contribution to Long-Term Sediment Budgets. *IAHS-AISH Publ.* **2008**, *325*, 114–122.
69. Mal'tsev, K.A.; Ivanov, M.A.; Sharifullin, A.G.; Golosov, V.N. Changes in the Rate of Soil Loss in River Basins within the Southern Part of European Russia. *Eurasian Soil Sci.* **2019**, *52*, 718–727. [[CrossRef](#)]
70. Walling, D.E.; Collins, A.L.; Sickingabula, H.M.; Leeks, G.J.L. Integrated Assessment of Catchment Suspended Sediment Budgets: A Zambian Example. *Land Degrad. Dev.* **2001**, *12*, 387–415. [[CrossRef](#)]
71. Walling, D.E.; Collins, A.L.; Sickingabula, H.M. Using Unsupported Lead-210 Measurements to Investigate Soil Erosion and Sediment Delivery in a Small Zambian Catchment. *Geomorphology* **2003**, *52*, 193–213. [[CrossRef](#)]
72. Walling, D.E. Human Impact on Land–Ocean Sediment Transfer by the World's Rivers. *Geomorphology* **2006**, *79*, 192–216. [[CrossRef](#)]
73. Blake, W.H.; Wallbrink, P.J.; Wilkinson, S.N.; Humphreys, G.S.; Doerr, S.H.; Shakesby, R.A.; Tomkins, K.M. Deriving Hillslope Sediment Budgets in Wildfire-Affected Forests Using Fallout Radionuclide Tracers. *Geomorphology* **2009**, *104*, 105–116. [[CrossRef](#)]
74. Navas, A.; López-Vicente, M.; Gaspar, L.; Palazón, L.; Quijano, L. Establishing a Tracer-Based Sediment Budget to Preserve Wetlands in Mediterranean Mountain Agroecosystems (NE Spain). *Sci. Total Environ.* **2014**, *496*, 132–143. [[CrossRef](#)] [[PubMed](#)]

75. Yermolaev, O.P.; Medvedeva, R.A.; Ivanov, M.A. Modern gully erosion in forest and forest-steppe landscapes of the east of the Russian Plain. *Geomorphology* **2021**, *52*, 28–41. [[CrossRef](#)]
76. Butakov, G.P.; Serebrennikova, I.A.; Yusupova, V.V. The Dynamics of Gully Erosion and River at the End of the 20th Century on the Territory of the Republic of Tatarstan. In *Modern and Ancient Erosion Processes*; Butakov, G.P., Larionov, G.A., Eds.; Kazan University: Kazan, Russia, 2001; pp. 51–67.
77. Gusarov, A.V.; Golosov, V.N.; Ivanov, M.M.; Sharifullin, A.G. Influence of Relief Characteristics and Landscape Connectivity on Sediment Redistribution in Small Agricultural Catchments in the Forest-Steppe Landscape Zone of the Russian Plain within European Russia. *Geomorphology* **2019**, *327*, 230–247. [[CrossRef](#)]
78. Chalov, R.S.; Sidorchuk, A.Y.; Golosov, V.N. (Eds.) *Catchment Erosion-Fluvial Systems: Monograph*; INFRA-M: Moscow, Russia, 2017.
79. Golosov, V.; Panin, A. Century-Scale Stream Network Dynamics in the Russian Plain in Response to Climate and Land Use Change. *Catena* **2006**, *66*, 74–92. [[CrossRef](#)]
80. Park, H.; Sherstiukov, A.B.; Fedorov, A.N.; Polyakov, I.V.; Walsh, J.E. An Observation-Based Assessment of the Influences of Air Temperature and Snow Depth on Soil Temperature in Russia. *Environ. Res. Lett.* **2014**, *9*, 064026. [[CrossRef](#)]
81. Petelko, A.I.; Golosov, V.N.; Belyaev, V.R. Experience of Design of System of Counter-Erosion Measures. In Proceedings of the 10th International Symposium on River Sedimentation, Moscow, Russia, 1–4 August 2007; Volume 1, pp. 311–316.
82. Golosov, V.N. Eroziionno-Akkumulyativnyye Protsessy Na Sklonakh v Yuzhnoy Chasti Nechernozemnoy Zony (Erosion-Accumulative Processes on Slopes in the Southern Part of the Non-Chernozem Zone). *Geomorphologiya* **1988**, *6*, 51–57.
83. Barabanov, A.T.; Dolgov, S.V.; Koronkevich, N.I.; Panov, V.I.; Petel'ko, A.I. Surface Runoff and Snowmelt Infiltration into the Soil on Plowlands in the Forest-Steppe and Steppe Zones of the East European Plain. *Eurasian Soil Sci.* **2018**, *51*, 66–72. [[CrossRef](#)]
84. Tsymbarovich, P.; Kust, G.; Kumani, M.; Golosov, V.; Andreeva, O. Soil Erosion: An Important Indicator for the Assessment of Land Degradation Neutrality in Russia. *Int. Soil Water Conserv. Res.* **2020**, *8*, 418–429. [[CrossRef](#)]
85. Moatar, F.; Meybeck, M.; Raymond, S.; Birgand, F.; Curie, F. River Flux Uncertainties Predicted by Hydrological Variability and Riverine Material Behaviour: Predicting uncertainties when monitoring riverine material fluxes. *Hydrol. Process.* **2013**, *27*, 3535–3546. [[CrossRef](#)]